Papaioannou George (Orcid ID: 0000-0002-7389-6640)

Running head: Sensitivity of Habitat Hydraulic Model Outputs to DTM and Computational Mesh Resolution

Sensitivity of Habitat Hydraulic Model Outputs to DTM and Computational Mesh Resolution

George Papaioannou*, Christina Papadaki, and Elias Dimitriou

Institute of Marine Biological Resources and Inland Waters, Hellenic Centre for Marine Research, 46,7 km Athens-Sounio, Mavro Lithari, Anavissos, Attiki, GR 19013, Greece.

* Correspondence: George Papaioannou, E-mail: gpapaioan@hcmr.gr

Abstract: In this study, a state-of-the-art approach in modelling fish habitats, using high-resolution topographical data, obtained from Unmanned Aerial Vehicle (UAV), was applied. Habitat Suitability Indices are used to predict how changes in discharge affect instream fish habitats. HSIs regarding depth and velocity for two size classes (small sized fish 5 –15 cm, Total Length (TL) and large sized >15 cm TL) of *Salmo pelagonicus* and *Barbus balcanicus*, were used, in combination with a two-dimensional (2D) hydraulic-hydrodynamic model, for the estimation of the Weighted Usable Area (WUA) in a mountainous stream. Computational mesh and/or DTM resolution selection may influence the accuracy of WUA results, especially in boulder and cobble-bed streams with complex habitat structures. The aim of the study is to examine the sensitivity of various hydraulic-hydrodynamic modelling geometry configurations on WUA at ungauged or poorly gauged streams. Comparisons of three different geometry configurations: 1) Identical computational mesh and DTM resolution (SensComb), 2) Finest computational mesh resolution combined with different DTM resolutions (SensDTM), 3) Finest DTM resolution combined with different computational mesh resolutions, as part of 2D hydrodynamic modelling, were applied to test the differences in WUA (SensMesh). WUA maps were generated for both fish species and class sizes for each modelling geometry configuration and compared to each other for assessing the sensitivity of the two-input data (computational mesh and DTM). Results provided by both indices, and their spatial distribution indicated the optimal DTM and computational mesh resolution as well as the sensitivity of a specific hydraulic-habitat model on them.

Keywords: habitat-hydraulic modelling; hydraulic-hydrodynamic model; sensitivity analysis; Weighted Usable Area; Habitat suitability indices models;

1. INTRODUCTION

River discharge modifications caused by anthropogenic actions may alter the natural flow regime of rivers (Overton et al., 2014; Poff & Schmidt, 2016; Poff, Tharme, & Arthington, 2017). There are numerous studies providing evidence about the consequences of these alterations, which cause environmental degradation and resources depletion (Acreman, 2016; Bunn & Arthington, 2002; Poff et al., 2010). Human needs for water are continually growing, indicating the priority that should be given by scientists and water managers on meeting environmental water needs. Fish habitat simulations with the use of hydraulic modelling have been increasingly used for environmental water assessments in line with the Water Framework Directive (WFD) of the European Union (Acreman & Ferguson, 2010). Habitat Suitability Index curves in combination with one (1D) and two (2D) dimensional hydrodynamic models are commonly used in studies to estimate the available habitat for the fish species and various flow scenarios (García, Jorde, Habit, Caamaño, & Parra, 2011; Kondolf, Larsen, & Williams, 2000; Lacey & Millar, 2004; Papadaki, Bellos, Ntoanidis, & Dimitriou, 2017; Papadaki, Bellos, Stoumboudi, Kopsiaftis, & Dimitriou, 2017; Tamminga, Hugenholtz, Eaton, & Lapointe, 2015). The capabilities of these models, for habitat modelling and accurate estimation of the flow characteristics, have been illustrated in many studies (Ahmadi-Nedushan, St-Hilaire, Bérubé, Ouarda, & Robichaud, 2008; Boavida, Santos, Katopodis, Ferreira, & Pinheiro, 2013; Gallagher & Gard, 1999; Lee, Kil, & Jeong, 2010; Mouton, Schneider, Depestele, Goethals, & De Pauw, 2007; Waddle, 2009). However, data availability has limited the applicability of habitat modelling to ungauged or poorly gauged mountainous streams with complex river and riparian areas (Benjankar, Tonina, & Mckean, 2015; Vezza, Parasiewicz, Spairani, & Comoglio, 2014). Thus, despite the increasing studies in the field, rapid and accurate habitat modelling remains a substantial challenge, especially for mountainous streams. This is due to the nature of the specific scientific field that is very complex and involves numerous parameters.

The part of habitat analysis that involves the hydraulic-hydrodynamic modelling includes several sources of uncertainty such as 1) Input data (e.g., initial and boundary condition data, hydraulic modelling geometry configuration, digital elevation model accuracy, roughness parameterization), 2) Model structure (1D, 2D, quasi 2D, 1D/2D), 3) Internal model parameters. Furthermore, the overall uncertainty of habitat hydraulic modelling process is influenced by the impact (significant or minor) of each type of uncertainty (Bates, Pappenberger, & Romanowicz, 2014). One of the main factors that affect the choice of the hydrodynamic modelling approach (1D, 2D, 1D/2D) is the complexity of the stream topography. Long stream reaches are usually processed with the use of a 1D hydraulic-hydrodynamic model, while in smaller stream reaches the use of 2D hydraulic-hydrodynamic models is preferred (Katopodis, 2012). Moreover, previous studies showed that in complex river topographies where flows have local variations (e.g., transverse flow and velocity gradient) the use of a 2D model is advantageous in comparison to the 1D model (Crowder & Diplas, 2000; Pasternack & Senter, 2013). 2D modelling is an emerging tool in the assessment of flow alteration effects associated with water resource projects and habitat modelling (Fabris et al., 2017; Jowett & Duncan, 2012; Leclerc, Boudreault, Bechara, & Corfa, 1995; van Oorschot, Kleinhans, Buijse, Geerling, & Middelkoop, 2018). However, the investigation of spatiotemporal variability of available habitats using 2D models can be affected by the data set and the methodology followed for the DTM generation which therefore affects the hydraulic characteristics and the habitat availability.

One of the most critical factors of uncertainty in hydraulic-hydrodynamic modelling applications is the Digital Terrain Model (DTM) accuracy. DTM generation cannot be accomplished without errors, especially in areas with compound terrains, and depends on the topographical methods used (Papaioannou, Loukas, Vasiliades, & Aronica, 2016; Tsubaki & Fujita, 2010). Ground surveying topographic approaches and photogrammetric methods are the most common techniques used for river geometry data collection and by extension the DTM generation. Despite the fact that these techniques are well established, when they are applied for hydraulic-hydrodynamic modelling applications, they are subject to certain limitations such as the time required for the measurements, the coverage of the study area, the point or pixel density, the accuracy of the derived data sets and the interpolation techniques that can create erroneous areas in the DTM (Md Ali, Solomatine, & Di Baldassarre, 2015; Teng, Vaze, Dutta, & Marvanek, 2015). These restrictive factors can be exceeded with the use of new spatial tools that produce high-resolution digital elevation models leading to better hydraulic-hydrodynamic model configurations and accurate fish habitat hydraulic modelling. Technological advancements in the last decade, have driven the use of Unmanned Aerial Vehicles (UAV) in many scientific fields (e.g. agriculture, mining and construction, natural hazards such as floods and fires) (SESAR, 2016). Recent studies have predicted a rapid increase in UAV usage in the near future**.** The usage of UAVs in habitat analysis and more specifically in habitat modelling is even more recent (Tamminga et al., 2015). A significant advantage of UAV, in comparison to common topographical methods, is the detailed information provided by digital orthophotos of the river and the riverine geometry which can improve the habitat modelling, especially in mountain streams with complex terrain (Dimitriou & Stavroulaki, 2018; Woodget, Austrums, Maddock, & Habit, 2017). On the other hand, UAV applications in hydraulic-hydrodynamic modelling require distinct skills and interdisciplinary knowledge. DSM and DTM are constructed using point cloud data and by using software programs (e.g. Pix4D) it is possible to produce them automatically. Nevertheless, in complex streams, point cloud classification is required to improve the DTM. If point cloud classification will not take place, all the points are treated as non-terrain points and the DTM is a smoothed version of the DSM (Pix4D, 2019).

Other important factors that can affect the results of a hydraulic-hydrodynamic model are the DTM and the computational mesh resolution that is named from now on as “mesh”. Several studies examined the effect of the mesh resolution in flood inundation modelling and mapping support the fact that the use of smaller mesh elements reduces the terrain truncation errors and flow truncation errors (Begnudelli & Sanders, 2007; Begnudelli, Sanders, & Bradford, 2008; Horritt, Bates, & Mattinson, 2006; Schubert, Sanders, Smith, & Wright, 2008). Moreover, numerous studies that examined the effect of the DTM accuracy and resolution in flood inundation modelling and mapping, support the fact that detailed and accurate representation of the river and riverine area has significant impact on the hydraulic-hydrodynamic modelling results, not only concerning the flood extent but the water depth as well (Courty, Soriano-Monzalvo, & Pedrozo-Acuña, 2019; Lim & Brandt, 2019; Md Ali et al., 2015; Papaioannou, 2017; Papaioannou, Loukas, & Georgiadis, 2013; Papaioannou et al., 2016; Vozinaki, Morianou, Alexakis, & Tsanis, 2017). Nevertheless, a limited number of studies in fish habitat hydraulic modelling have examined the DTM and/or mesh resolution (Boavida et al., 2013; Crowder & Diplas, 2000; Grantham, 2013; Kolden, Fox, Bledsoe, & Kondratieff, 2016; Lin, Lin, & Wu, 2015). Despite the importance of the DTM and/or mesh resolution, there is a gap in the implementation of a detailed sensitivity analysis to examine the impacts of different hydraulic-hydrodynamic modelling geometry configurations (DTM and/or mesh resolution) on fish habitat hydraulic modelling, at mountainous streams with complex river and riverine areas.

In this study, we tested the impact of different hydraulic-hydrodynamic modelling geometry configurations (DTM and/or mesh resolution) on fish habitat - hydraulic modelling, at a poorly gauged mountainous stream focusing on two fish species *Salmo pelagonicus* (here after trout) and *Barbus balcanicus* (hereafter barbel). The aim of the study is to assess the sensitivity of various hydraulic-hydrodynamic modelling geometry configurations (DTM and/or Mesh resolution) on WUA index (habitat hydraulic modelling) at ungauged or poorly gauged streams. Therefore, three different hydraulic-hydrodynamic modelling geometry configurations are used. The methodology is based on the use of high-resolution topographical data obtained from UAV, habitat suitability analysis using depth and velocity HSIs and the Weighted Usable Area (WUA) index, for two size classes of two endemic fish species of the Balkans, and a two-dimensional (2D) hydraulic-hydrodynamic model. The selected study area of Drosopigi stream, Florina, Greece, is characterized as ungauged or poorly gauged mountainous stream with complex river and riverine areas.

2. STUDY AREA

Axios river is located in the central Balkan Peninsula. The river drains 80% of North Macedonia, 12% of Greece and small parts of Bulgaria and Serbia. The river is hydrologically connected to Lake Doirani (Dojran), shared between Greece and North Macedonia (Dimitriou, Panagiotopoulos, Mentzafou, & Anagnostou, 2018). The river catchment is covering an area of approximately 25,000 km^2. The annual average natural water discharge of the Axios River is 159 m^3/sec. The Greek watershed is approximately 849.4 km^2. The major land use is agricultural (48.4%), and the main land cover is forests and semi-natural areas (48.7%) based on CORINE Land Cover (European Environmental Agency, 2012). In this research effort a 450 m river segment of one of the mountainous Axios tributaries, located in the Greek watershed (mean altitude at 950 a.s.l. 40.680300°, 21.448573°, WGS 84), named Drosopigi was selected as study area (Figure 1). The river segment under study is part of Drosopigi stream, and it formulates a pool-riffle channel (morphologic definitions of Buffington, Montgomery, & Greenberg, (2004); Montgomery & Buffington, (1997)). The river bed is mainly composed of cobbles and boulders that are uniformly spatial distributed within the riverbed. According to the regular flow of 0.8 m^3/sec, the approximate median value of the width is 7 m (ranges from 3.8 to 14.8 m) and the depth is 0.2 m (ranges from 0 to 1.45 m).

3. MATERIAL AND METHODS

In this study, a sensitivity analysis is applied to examine the effect of different DTM and/or mesh resolutions for fish habitat-hydraulic modelling and mapping. Figure 2 presents the flow chart of input data preparation and the methodology followed for the sensitivity analysis. Red dashed lines depict the processes followed in the field data collections section (3.1), and green dashed lines enclose the processes followed in the Hydraulic-Hydrodynamic model section (3.2) and the remaining elements comprise the Habitat-Hydraulic modelling section (3.3) (Figure 2). The sensitivity analysis methodology uses three different scenarios: 1) SensComb, 2) SensDTM, 3) SensMesh (detailed analysis of the scenarios is presenting in section 3.2). The methodology described in the next paragraphs is used to identify the sensitivity of habitat hydraulic model outputs to DTM and/or computational mesh changes.

3.1. Field Data Collection

The field topographic data in the study area (Drosopigi river) were collected in 5/4/2017 by using a DJI Phantom 3 Professional UAV to capture overlapping pictures that were then introduced in the Pix4D mapper software to apply photogrammetric algorithms and develop the area's Digital Surface Model (DSM) and the Digital Terrain Model (DTM). The resolution of each picture was 4000x3000 pixels and the percentage overlap for adjacent pictures was 80%. The area covered in the field survey was approximately 710 m x 210 m (length x width) along the river course, and the flight altitude was 70 m. The Pix4D photogrammetric process steps include the estimation of the UAV's camera parameters for image calibration and bundle adjustment, the extraction of identical image points (tie points) between the overlapping pictures, the estimation of the 3D point cloud and the built up of the DSM. The photogrammetry algorithms are analytically described in Unger, Pock, Grabner, Klaus, & Bischof (2009), while the mean error of the reconstructed surface is approximately 1-3 times the Ground Sampling Distance (Küng et al., 2012). The cell size of the produced DTM was approximately 0.03 m which correspond to a potential inherent error between 0.03 m and 0.09 m. The number of 2D keypoints observations used by the photogrammetric algorithm (matched in at least two images) are 1,063,617 while the number of 3D points generated is 400,708. The mean reprojection error in pixels is 1.81 (0.055 m) which is within the acceptable limits of UAV generated DTMs (Dimitriou & Stavroulaki, 2018).

Regarding the camera position and orientation uncertainties, the mean potential errors are lower than 0.14 m in X-Y dimensions and less than 0.25 m in the Z dimension (Table 1). Moreover, given the aforementioned, potential errors which were significantly lower than the pixel size of the finer DTM used in this study (0.15 m), the accuracy of the DTM generation approach can be considered satisfactory. The aforementioned error analysis refers to the relative, internal errors of the photogrammetric process as estimated by the Pix4D software, since no Ground Control Points were collected. Therefore, the absolute errors in the resulted DTM could be higher but since the same DTM output is intended to be used in all hydraulic model scenarios the comparative assessment is going to be valid. Regarding the capture of the river bathymetry, several studies indicated that UAV-based aerial photos are appropriate for optical bathymetric modelling (Javernick, Brasington, & Caruso, 2014; Williams, Brasington, Vericat, & Hicks, 2014) and in this case study the low depth of the water, as well as its clarity, contributed to the adequate estimation of the submerged terrain. The Pix4D uses image classification techniques to map the vegetation cover which then subtracts from the produced DSM, to provide the DTM which was used in the specific case study. The coordinate system used was the World Geodetic System 1984 UTM Zone 34N (WGS84) while the ArcMap software was used for resampling (Nearest neighbor assignment) the detailed produced DTM to more coarse spatial resolution.

Finally, other potential sources of DTM are the National Cadastre and Mapping Agency S.A. (NCMA) DTM (pixel size 5m) and the SRTM (pixel size 30m) that have coarse resolution fluctuating from 5 to 30 meters with the absolute accuracy to vary from ≤3.92 m and ±16 m respectively (Elkhrachy, 2018; Papaioannou et al., 2018). Recognising the importance for a detailed and accurate representation of the river and riverine area and based on the above-mentioned absolute accuracies of the DTMs and the stream characteristics (typical mountain stream with variable width of about 3.8 to 14.8 m), the UAV DTM is used for fish habitat hydraulic modelling.

3.2. Hydraulic-Hydrodynamic Model

The hydrodynamic characteristics of the study area were simulated by a two-dimensional (2D) hydrodynamic model (HEC-RAS). HEC-RAS model is one of the most acknowledged hydraulic-hydrodynamic models worldwide, developed by the Hydrologic Engineering Center (HEC) of United States Army Corps of Engineers. Despite the recent (official release in 2016) development of the two-dimensional (2D) HEC-RAS model, it is already used in many hydraulic-hydrodynamic modelling applications (Afshari et al., 2018; Papaioannou et al., 2018; Patel, Ramirez, Srivastava, Bray, & Han, 2017; Vozinaki et al., 2017; Wang et al., 2018). Furthermore, the U.S. Army Corps of Engineers conducted a benchmark analysis and examined the capabilities of the HEC-RAS two-dimensional modelling. The U.S. Army Corps of Engineers benchmark analysis provides evidence that the performance of 2D HEC-RAS is remarkable and can produce similar results to the leading 2D models (Brunner & CEIWR-HHT, 2018; Brunner, Sanchez, Molls, & Parr, 2018). Therefore, the 2D HEC-RAS hydraulic-hydrodynamic model selected for fish habitat hydraulic modelling.

The two-dimensional (2D) HEC-RAS 5.0.3 computational engine solves either the full 2D Saint-Venant equations or the 2D diffusive wave equations using an implicit finite volume algorithm (Brunner & CEIWR-HHT, 2018). Despite the relatively higher computational demand, the full 2D Saint-Venant equations, were used in this study, in order to capture the flow alterations between pools and riffles, and around the boulders (complex river terrain). The 2D HEC-RAS model set up consists of the generation of the Terrain, the creation of the computational mesh, the determination of upstream and downstream boundary conditions and the selected Manning roughness values. All parameters of the two dimensional (2D) HEC-RAS model, except the 2D hydraulic-hydrodynamic modelling geometry and the Terrain, were set as constant and determined respectively, in agreement with HEC-RAS standards (Brunner, 2016; Brunner & CEIWR-HEC, 2016a, 2016b; Brunner, Warner, Wolfe, Piper, & Marston, 2016). In this study, the generated computational meshes are approximately homogenous (structured mesh). In Table 2 the mesh sizes used (0.3 m to 3 m) are presented. UAV high-resolution orthophotos were used for the generation of the high accuracy DTM (pixel size of 0.15 m). Through the resampling process, the high-resolution DTM was converted to coarser spatial resolutions. The configuration of the upstream boundary condition is based on the representative discharge of 0.8 m^3/sec while the downstream boundary condition determined as normal water depth or energy slope (Brunner, 2016; Brunner & CEIWR-HEC, 2016a, 2016b; Brunner et al., 2016). Recent studies suggest the use of steady flow simulation for the evaluation of hydraulic model performance (Dimitriadis et al., 2016; Horritt & Bates, 2002). Hence, the inflow (0.8 m^3/sec) was set as constant for the simulations in order to achieve steady-state conditions. Another important factor in hydraulic-hydrodynamic modelling is the determination of the computational step. Stability and accuracy can be achieved, in 2D HEC-RAS modelling that uses the full 2D Saint-Venant equations, when the selected time step satisfies the Courant Condition (Brunner & CEIWR-HEC, 2016a):

$$C_r = V_w * (\Delta t / \Delta x) \leq 1 \text{ (with a max } C = 3) \tag{1}$$

where C_r is the Courant Number; V_w is the wave celerity (m/s); Δt is the computational time step (s); Δx is the average cell size (m).

Therefore, the computation interval was set constant to 0.2 sec for all simulations. The determination of Manning's roughness coefficient was based on a semi-automated calibration process. The calibration process is based on an adapted form of the code that is presented in the book of Goodell (2014) and the study of Ederle (2017). The main core of the calibration process is based on the handling of the HEC-RAS model using Excel Visual Basic for Applications (VBA) routines. Thus, the calibration process is based on an iterative modelling procedure where after a single simulation, a new roughness coefficient value is selected for iterative modelling. The entire process is terminated when the number of realizations meets the number of the given roughness n values. Therefore, one hundred (100) simulations are implemented using different Manning roughness n values with values that have three (3) digits after the decimal point and ranges from 0.02 to 0.12. In order to eliminate the differences between the observed and the simulated water depth value, further detailed analysis that focused on specific range of Manning roughness n values (i.e. 0.0770 to 0.0790), with values that have four (4) digits after the decimal point, is conducted. Thus, the selection of the best-fitted roughness value is based on the comparison between the observed water level (gauged station data) and the simulated one for the user-defined validation pixel (gauged station location). In this study, the model was calibrated for a discharge of 0.44 m^3/sec by adjusting the bed channel roughness until good agreement of simulated versus observed water level was achieved. The estimation of the discharge value of 0.44 m^3/sec is based on the velocity - area method (Buchanan & Somers, 1976). The data used for the discharge estimation retrieved from two cross sections close to the gauged station. Furthermore, the estimation of the average velocity is based on the assumption that the mean velocity is observed at the 60% of the maximum depth for water depths lower than 0.76 m and at 20% and 80% of the maximum depth for water depths greater than 0.76 m (Buchanan & Somers, 1976; Mosley & McKerchar, 1993). Due to lack of data, the selected discharge (0.44 m^3/sec) is the only discharge measurement that is associated with the water level measurements (gauged station data) of the study area. Moreover, the finest DTM (0.15 m) and mesh (0.3 m) resolutions were used in the calibration process. Finally, according to the calibration procedure, the Manning's roughness coefficient value was set to 0.0782 for the entire fish habitat-hydraulic modelling stream reach. The validity of the selected Manning's roughness coefficient value was examined by comparing the selected value against the result of the Loukas & Quick (1996) roughness coefficient empirical formula. The Loukas & Quick (1996) empirical formula is based on data retrieved from high gradient natural channels with cobble and boulder bed materials and is expressed as:

$$n = 0.0326+1.3041S_w \tag{2}$$

where *n* is the Manning's roughness coefficient; S_w is the water surface slope.

The assumption that the water surface slope is the same with the river bed slope has been previously used for the estimation of the roughness coefficient in Loukas & Quick (1996) formula. This assumption is acceptable when channel slopes are averaged over longer distances of the order of hundreds of meters (Hughes, 1993). According to the UAV generated DTM, the gradient of the stream reach is approximately 0.034 which means that the altitude is rising approximately 3.4 m every 100 m (length). Thus, the estimated value of the roughness coefficient by the Loukas & Quick (1996) formula is 0.077.

Finally, three (3) different hydraulic-hydrodynamic geometry configuration sets have been established for the sensitivity analysis (Table 3). These are: 1) **SensComb** – Mesh and DTM resolution are identical (DTM pixel resolution and mesh element size varies from 0.3 m to 3 m), 2) **SensDTM** – Finest mesh resolution (0.09 m^2 average mesh element size) is combined with different DTM resolutions (DTM pixel resolution varies from 0.3 to 3 m), 3) **SensMesh** - Finest DTM resolution (DTM pixel resolution of 0.15 m) is combined with different mesh resolutions (Average mesh element size varies from 0.09 m^2 to approximately 9 m^2).

3.3. Habitat-Hydraulic Modelling

Simulation of physical habitat is accomplished using hydraulic simulation and habitat simulation. Hydraulic simulation provides information regarding water surface elevation and velocity for a certain discharge (Choi, Jung, & Kim, 2015). In this study two size classes of two fish species; Salmo pelagonicus and Barbus balcanicus: small sized fish 5 –15 cm, Total Length (TL) and large sized >15 cm TL were used as target species. These species are endemic of the Balkan rivers and the most abundant or the only fish species, in the upper section of the Drosopigi stream. Both fish species have been negatively impacted from hydromorphological alterations and illegal water abstractions (Barbieri et al., 2015), while they both being rheophilic, potamodromous species that require specific rheolithophilic conditions for reproduction (Zogaris et al., 2018). Nevertheless, Barbus balcanicus is considered to have a lower response to hydromorphological changes than the cold-water trout species.

Habitat – hydraulic modelling has been widely used to estimate Weighted Usable Area (WUA) for environmental water requirements (Benjankar et al., 2015; Leclerc et al., 1995). WUA is an index determining the relationship between the physical habitat (depth, velocity) and flow, based on HSIs. WUA is the sum of a composite HSI weighted by area, over all the points of the hydrodynamic model in the study site. The composite HSI for depth and velocity is estimated using the product method. The product method assumes that fish select each particular variable independently of the rest (depth, velocity) and therefore to estimate the composite HSI, a multiplication of the different variables' suitability indices was applied (Bovee et al., 1998). Where Ci is the composite HSI, and Ai is the cell area.

$$WUA = \sum_{i=1}^{n} Ai \;\; x \;\; Ci \tag{3}$$

More specifically, one discharge (0.8 m^3/sec) was selected as representative discharge value of the summer conditions in the study area (June to September) based on E-HYPE Pan-European hydrological model (Arheimer, Wallman, Donnelly, Nyström, & Pers, 2011; SMHI-HYPEweb, 2018). WUA was used to quantify the differences in habitat suitability results based on various resolutions and combinations of the DTM and/or the mesh. In addition, to study only the conditions with high suitability a threshold WUA index (hereafter $WUA_{0.5}$) considering the cells with combined habitat suitability higher than 0.5 (Kolden et al., 2016; Papadaki et al., 2016) was also estimated for the two fish species. Univariate HSIs for depth and velocity were developed in a previous study (Papadaki, Bellos, Stoumboudi, et al., 2017) following standard procedures (Bovee, 1986). The estimated HSIs values converted in Geographical Information System (GIS) "friendly" data format (.dbf) using R software (R Core Team, 2014). Then, the converted HSIs results were imported into ArcMap for the generation of the spatial distributed WUA and $WUA_{0.5}$ using specific models-scripts created in the ArcMap ModelBuilder environment.

4. RESULTS AND DISCUSSION

A sensitivity analysis on habitat modelling was applied for different DTM and/or mesh spatial resolution configurations focusing on two fish species. The estimation of WUA indices was accomplished using the derived velocities and water depths of 2D Hydraulic-hydrodynamic model (HEC-RAS) for the *Salmo pelagonicus* (trout) and the *Barbus balcanicus* (babrel). Several hydraulic-hydrodynamic model geometries were used (DTM and/or mesh resolution) to investigate the effect of DTM and/or mesh resolution on WUA and $WUA_{0.5}$.

An important finding revealed from Figure 3 concerning the variations of water depth and velocity is that the turning point for all study scenarios is at 1m. Thus, water depth and velocity provide similar median values for resolutions finer than 1m. As expected, water depth has smaller variations comparing to the velocity with the increase of the DTM and/or Mesh resolution (Figure 3). Specifically, the median water depth values for all the examined scenarios are ranging between 0.2 m and 0.22 m while the median velocity values for all the examined scenarios are ranging between 0.5 m/s and 0.56 m/s. Thus, the differences of the median water depth are 0.02 m and the differences of the median velocity are 0.06 m/s.

Table 4 presents the WUA, and $WUA_{0.5}$ values for all examined DTM and/or mesh configurations and all fish species, while a visual representation of Table 4 is presented in Figure 4 as Box and Whisker Plots. Even though the results of WUA differ from $WUA_{0.5}$, both indices have a similar response in the three geometry scenarios. $WUA_{0.5}$ index provided wider interquartile ranges than WUA index for all examined scenarios The analysis of WUA (Table 4, Figure 4) showed that the interquartile ranges (1st quartile -25% to the 3rd quartile 75%) are not equally distributed, with the majority of the grid cells to participate in the 1st quartile (approximately 80% of the total interquartile range) for all examined scenarios.

An important finding revealed from Table 4, and Figure 4 concerning the hydraulic-hydrodynamic modelling geometry configuration is that SensComb is the scenario with the biggest variations in WUA and $WUA_{0.5}$ (variation of the WUA ranged from 756 to 2120 and $WUA_{0.5}$ from 356 to 1632). In SensComb and SensMesh scenarios, the distribution of WUA and $WUA_{0.5}$ is following approximately the same pattern (Table 4, Figure 4). Specifically, in the SensComb scenario, WUA and $WUA_{0.5}$ median values range from 1474 to 1970 and from 907 to 1381, respectively and in the SensMesh scenario, WUA, and $WUA_{0.5}$ median values vary from 1496 to 1712 and from 912 to 1112, respectively. Also, the same pattern is approximately followed for both quartiles (25% and 75%) and the interquartile of SensComb and SensMesh scenarios, where an increase of the quartiles and interquartile values is observed for both indices with the rise of the pixel/mesh resolution (Table 4, Figure 4). Thus, it is observed in SensComb and SensMesh scenarios that WUA and $WUA_{0.5}$ indices become more sensitive with the rise of the DTM and/or mesh resolution (Table 4, Figure 4). Significantly, SensDTM scenario seems to be approximately immune in the resolution changes, based on the median and the corresponding quartiles values for both WUA and $WUA_{0.5}$, with the turning point in 3 m resolution (Table 4, Figure 4). Moreover, the interquartile range is ascending from the SensDTM to the SensMesh and then to the SensComb scenario for both examined indices (WUA and $WUA_{0.5}$) (Table 4, Figure 4). The most remarkable result that emerges from the analysis is that the turning point of WUA and $WUA_{0.5}$ is approximately from 1 m DTM and/or mesh resolution and above, where a stronger rising tendency exists (Table 4, Figure 4, Figure 5). Therefore, the value of one (1) meter could be proposed as an upper threshold limit in DTM and/or mesh resolution for a better approximation of WUA and $WUA_{0.5}$ for the examined fish species and sizes (Table 4, Figure 4, Figure 5). Furthermore, it is interesting to note that, based on the median values of both indices (WUA and $WUA_{0.5}$), the DTM and/or mesh resolution of 0.3 m gives approximately the same results for all geometry scenarios (Figure 4, Figure 5). These findings highlight the importance of the DTM accuracy and/or mesh accuracy in habitat modelling efficiency.

The evaluation of spatial distributed WUA and $WUA_{0.5}$ is based on the spatially distributed HSIs (Figure 6). Therefore, similar spatial patterns are recognized between the different resolutions within each examined scenario for all scenarios (Figure 6). Despite the DTM resolution changes, an almost common spatial pattern of WUA is observed within the SensDTM scenario (Figure 6). Furthermore, an interesting outcome is that the SensComb and SensMesh scenarios are giving wider areas for values under the WUA threshold level of 0.5 as the resolution increased (Figure 6). Thus, the pattern of HSIs for both selected resolutions is similar, but the values close to the optimum HSIs values seems to affect the neighboring cells (Figure 6). Additionally, observations from high resolution results (e.g., DTM and/or mesh resolution 0.3 m) reveal a similar spatial pattern of WUA values among the same fish species and sizes between the geometry scenarios. On the other hand, in lower spatial resolutions (e.g., DTM and/or mesh resolution 1.6 m) some differences are observed in the spatial pattern of WUA values among the same fish species and sizes for the different hydraulic-hydrodynamic geometry scenarios (Figure 6). Considering the spatial distribution of WUA index, Barbel seems to prefer lateral habitats (closer to the banks of the stream), while Trout occupied habitats that exist in the center of the stream (where pools exist) (Figure 6). Also, by accounting Small Barbel microhabitat positions the majority of the additional pixels from the hydrodynamic model consist of low HSIs values while the pixels with optimum HSIs values have significant dispersion within the study area (Figure 6).

In Figure 7 a graphical representation of WUA and $WUA_{0.5}$ values, for all hydraulic-hydrodynamic geometry configurations and both fish species and sizes is presented. WUA index values estimated based on the habitat requirements of the Large Barbel are lower than those regarding the Large Trout. While $WUA_{0.5}$ values are approximately the same for the aforementioned fish species and sizes (Figure 7). WUA results for Small Trout and Large Barbel are similar as expected, since their habitat requirements are almost the same. While there is a substantial difference between the Small Trout and Large Barbel regarding $WUA_{0.5}$ index (Figure 7). In all examined scenarios Small Barbel WUA values are the lowest. It is important to note that, based on both indices (WUA and $WUA_{0.5}$), in SensDTM scenario, all fish species are almost immune to resolution changes with the turning point at 2.5 m (Figure 7). WUA and $WUA_{0.5}$ values are rising as the pixel/mesh resolution rises for all study scenarios and fish species and sizes (Figure 7). Nevertheless, WUA and $WUA_{0.5}$ values of Small Barbel appear to be immune to resolution changes for the SensMesh scenario. Finally, the lowest values of WUA and $WUA_{0.5}$ for all fish species and sizes are observed in SensDTM scenario.

5. CONCLUSIONS

In this paper, high-resolution topographical data collected with Unmanned Aerial Vehicle (UAV), were used in habitat - hydraulic modelling to estimate differences in habitat availability using WUA and $WUA_{0.5}$ indices. $WUA_{0.5}$ threshold index was chosen as an alternative scenario to be investigated mainly because the productive capacity of small areas with optimum habitat is different from the large areas of less than optimum habitat (Scott & Shirvell, 1987). Nevertheless, validation studies should be conducted in the future to be able to verify these results. The proposed methodology is developed for poorly gauged or ungauged mountainous streams with complex terrain. The HSIs of depth and velocity for two size classes of two endemic fish species of the Balkans were combined with the results (simulated water depth and velocity) of a two-dimensional (2D) hydraulic-hydrodynamic model, in order to estimate the WUA and $WUA_{0.5}$ indices. Several sensitivity analysis configurations were implemented due to the impact of DTM and/or mesh resolution in the estimated WUA and $WUA_{0.5}$ values. Then, WUA and $WUA_{0.5}$ maps were generated for both fish species and sizes for each modelling geometry configuration and compared for assessing the sensitivity of the selected input data (DTM and mesh resolution), at a mountainous stream of Florina, Greece.

WUA threshold indices are used in ecological flow studies (Capra, Breil, & Souchon, 1995; Papadaki et al., 2016). In this study both WUA and $WUA_{0.5}$ indices were used to analyze differences between the examined scenarios. Based on our aggregated results for all fish, the $WUA_{0.5}$ extent was similar to WUA since approximately 60% of the study area has combined HSIs values higher than 0.5. Moreover, the $WUA_{0.5}$ trends in the simulated scenarios were similar to WUA ones (Figure 5, Table 4).

From the three hydraulic-hydrodynamic modelling geometry configurations the SensComb scenario is affecting mostly the WUA and $WUA_{0.5}$ indices following by the SensMesh scenario (there is a positive tendency of the median and the interquartile range with the increase of the resolution) (Table 4, Figure 4, Figure 7). The SensDTM scenario is approximately immune to resolution changes (Table 4, Figure 4, Figure 7). Results from this study indicate that spatial resolutions finer than (1) meter have small impact on the final results and provide acceptable accuracy in habitat modelling applications. Thus, it is suggested that the resolution of the DEM and mesh should be limited to values lower or equal to one (1) meter. Moreover, it is interesting to note that the mesh resolution has a stronger impact on WUA in comparison to the DEM resolution.

Our results share some similarities with the Moore & Gregory (1988) findings where lateral habitats exist and are critical for specific fish species (Benjankar, Tonina, Sohrabi, & McKean, 2018). The existence of lateral habitats can be highlighted with the use of two-dimensional hydraulic-hydrodynamic models due to their capability to accurately reproduce the spatial flow patterns, especially for complex river and riverine areas (Alaska Energy Authority, 2012; Brown & Pasternack, 2009; Crowder & Diplas, 2000; Leclerc et al., 1995; Moore & Gregory, 1988). As expected the simulation time is connected with the DTM and/or mesh resolution and increase with finer resolution. Even though a complex hydraulic-hydrodynamic model (two-dimensional) is expected to give higher simulation times and usually requires increased computational resources, nowadays with the technological advancement in computer sciences, it can be implemented on desktop PCs (Papadaki et al., 2016; Pasternack & Senter, 2013). Accordingly, the findings of this study are consistent with previous results (Crowder & Diplas, 2000; Pasternack & Senter, 2013; Tonina & Jorde, 2013) where the use of a 2D hydraulic-hydrodynamic model can provide acceptable results for habitat modelling applications at boulder and cobble-bed streams with complex terrain.

Further investigation is needed in other regions with similar conditions in order to verify and generalize the presented findings. This paper has highlighted the importance of high-resolution topographical data in habitat modelling studies and the examination of several hydraulic-hydrodynamic modelling geometry configurations before the selection of the most appropriate one for habitat modelling. Finally, application of the proposed techniques in Drosopigi stream showed that sensitivity analysis should be a compulsory process in habitat suitability modelling. The employed methodology could be applied in areas with complex river and riverine terrain using typical physical habitat analysis techniques for habitat modelling.

ACKNOWLEDGMENTS

CONFLICTS OF INTEREST

The authors declare no conflict of interest.

REFERENCES

Acreman, M. (2016). Environmental flows-basics for novices. *Wiley Interdisciplinary Reviews: Water*, *3*(5), 622–628. https://doi.org/10.1002/wat2.1160

Acreman, M., & Ferguson, A. (2010). Environmental flows and the European Water Framework Directive. *Freshwater Biology*, *55*(1), 32–48. https://doi.org/10.1111/j.1365-2427.2009.02181.x

Afshari, S., Tavakoly, A. A., Rajib, M. A., Zheng, X., Follum, M. L., Omranian, E., & Fekete, B. M. (2018). Comparison of new generation low-complexity flood inundation mapping tools with a hydrodynamic model. *Journal of Hydrology*, *556*, 539–556. https://doi.org/10.1016/j.jhydrol.2017.11.036

Ahmadi-Nedushan, B., St-Hilaire, A., Bérubé, M., Ouarda, T. B. M. J., & Robichaud, É. (2008). Instream flow determination using a multiple input fuzzy-based rule system: a case study. *River Research and Applications*, *24*(3), 279–292. https://doi.org/10.1002/rra.1059

Alaska Energy Authority. (2012). *Fluvial Geomorphology Modeling*. Retrieved from http://www.susitna-watanahydro.org/documents/AEA_SuWa_FluvialModelingTechMemo20120518_Draft.pdf

Arheimer, B., Wallman, P., Donnelly, C., Nyström, K., & Pers, C. (2011). E-HypeWeb: Service for Water and Climate Information - and Future Hydrological Collaboration across Europe? In *9th International Symposium on Environmental Software Systems (ISESS)* (pp. 657–666). https://doi.org/10.1007/978-3-642-22285-6_71

Barbieri, R., Zogaris, S., Kalogianni, E., Stoumboudi, M. T., Chatzinikolaou, Y., Giakoumi, S., … Economou, A. (2015). *Freshwater Fishes and Lampreys of Greece*.

Bates, P. D., Pappenberger, F., & Romanowicz, R. J. (2014). Uncertainty in Flood Inundation Modelling. In *Applied Uncertainty Analysis for Flood Risk Management* (pp. 232–269). https://doi.org/10.1142/9781848162716

Begnudelli, L., & Sanders, B. F. (2007). Simulation of the St . Francis Dam-Break Flood. *Journal of Engineering Mechanics*, *133*(11), 1200–1212. https://doi.org/10.1061/(ASCE)0733-9399(2007)133:11(1200)

Begnudelli, L., Sanders, B. F., & Bradford, S. F. (2008). Adaptive Godunov-Based Model for Flood Simulation.

Journal of Hydraulic Engineering, *134*(6), 714–725. https://doi.org/10.1061/(ASCE)0733-9429(2008)134:6(714)

Benjankar, R., Tonina, D., & Mckean, J. (2015). One-dimensional and two-dimensional hydrodynamic modeling derived flow properties: Impacts on aquatic habitat quality predictions. *Earth Surface Processes and Landforms*, *40*(3), 340–356. https://doi.org/10.1002/esp.3637

Benjankar, R., Tonina, D., Sohrabi, M., & McKean, J. (2018). A virtual ecohdraulic watershed: integrating physical and biological variables to quantify aquatic habitat quality, (November), 1–14. https://doi.org/10.1002/eco.2062

Boavida, I., Santos, J. M., Katopodis, C., Ferreira, M. T., & Pinheiro, A. (2013). Uncertainty In Predicting The Fish-Response To Two-Dimensional Habitat Modeling Using Field Data. *River Research and Applications*, *29*(9), 1164–1174. https://doi.org/10.1002/rra.2603

Bovee, K. (1986). *Development and evaluation of habitat suitability criteria for use in the instream flow incremental methodology*. Washington, D.C. Retrieved from http://pubs.er.usgs.gov/publication/70121265

Bovee, K., Lamb, B., Bartholow, J., Stalnaker, C., Taylor, J., & Henriksen, J. (1998). *Stream habitat analysis using the instream flow incremental methodology*. Fort Collins, CO: U.S. Geological Survey.

Brown, R. A., & Pasternack, G. B. (2009). Comparison of methods for analysing salmon habitat rehabilitation designs for regulated rivers. *River Research and Applications*, *25*(6), 745–772. https://doi.org/10.1002/rra.1189

Brunner, G. W. (2016). HEC-RAS River Analysis System - Hydraulic Reference Manual, Version 5.0. US Army Corps of Engineers–Hydrologic Engineering Center. Retrieved from http://www.hec.usace.army.mil/software/hec-ras/documentation/HEC-RAS 5.0 Reference Manual.pdf

Brunner, G. W., & CEIWR-HEC. (2016a). HEC-RAS River Analysis System 2D Modeling User ' s Manual. US Army Corps of Engineers – Hydrologic Engineering Center. Retrieved from http://www.hec.usace.army.mil/software/hec-ras/documentation/HEC-RAS 5.0 2D Modeling Users Manual.pdf

Brunner, G. W., & CEIWR-HEC. (2016b). HEC-RAS River Analysis System User's Manual. US Army Corps of Engineers–Hydrologic Engineering Center. Retrieved from https://www.hec.usace.army.mil/software/hec-ras/documentation/HEC-RAS 5.0 Users Manual.pdf

Brunner, G. W., & CEIWR-HHT. (2018). Benchmarking of the HEC-RAS Two-Dimensional Hydraulic Modeling Capabilities. US Army Corps of Engineers – Hydrologic Engineering Center. Retrieved from http://www.hec.usace.army.mil/software/hec-ras/documentation/RD-51_Benchmarking_2D.pdf

Brunner, G. W., Sanchez, A., Molls, T., & Parr, D. A. (2018). HEC-RAS Verification and Validation Tests. US Army Corps of Engineers–Hydrologic Engineering Center. Davis, CA: Water Resources Hydrologic Engineering Center. Retrieved from https://www.hec.usace.army.mil/software/hec-ras/documentation/RD-52_HEC-RAS Verification and Validation.pdf

Brunner, G. W., Warner, J. C., Wolfe, B. C., Piper, S. S., & Marston, L. (2016). HEC-RAS River Analysis System Applications Guide. US Army Corps of Engineers–Hydrologic Engineering Center. Retrieved from https://www.hec.usace.army.mil/software/hec-ras/documentation/HEC-RAS 5.0 Applications Guide.pdf

Buchanan, T. J. J., & Somers, W. P. P. (1976). *Discharge measurements at gaging stations*. Retrieved from https://pubs.usgs.gov/twri/twri3a8/pdf/TWRI_3-A8.pdf

Buffington, J. M., Montgomery, D. R., & Greenberg, H. M. (2004). Basin-scale availability of salmonid spawning gravel as influenced by channel type and hydraulic roughness in mountain catchments. *Canadian Journal* *of Fisheries and Aquatic Sciences*, *61*(11), 2085–2096. https://doi.org/10.1139/f04-141

Bunn, S. E., & Arthington, A. H. (2002). Basic principles and ecological consequences of altered flow regimes for aquatic biodiversity. *Environmental Management*, *30*(4), 492–507. https://doi.org/10.1007/s00267-002-2737-0

Capra, H., Breil, P., & Souchon, Y. (1995). A NEW TOOL TO INTERPRET MAGNITUDE AND DURATION OF FISH HABITAT VARIATIONS. *REGULATED RIVERS: RESEARCH & MANAGEMENT*, *10*, 281–289. https://doi.org/10.1002/rrr.3450100221

Choi, S. U., Jung, S., & Kim, S. K. (2015). A quasi-2D and quasi-steady hydraulic model for physical habitat simulations. *Ecohydrology*, *8*(2), 263–272. https://doi.org/10.1002/eco.1504

Courty, L. G., Soriano-Monzalvo, J. C., & Pedrozo-Acuña, A. (2019). Evaluation of open-access global digital elevation models (AW3D30, SRTM, and ASTER) for flood modelling purposes. *Journal of Flood Risk Management*, *12*(April), 1–14. https://doi.org/10.1111/jfr3.12550

Crowder, D. W., & Diplas, P. (2000). Using two-dimensional hydrodynamic models at scales of ecological importance. *Journal of Hydrology*, *230*(3–4), 172–191. https://doi.org/10.1016/S0022-1694(00)00177-3

Dimitriadis, P., Tegos, A., Oikonomou, A., Pagana, V., Koukouvinos, A., Mamassis, N., … Efstratiadis, A. (2016). Comparative evaluation of 1D and quasi-2D hydraulic models based on benchmark and real-world applications for uncertainty assessment in flood mapping. *Journal of Hydrology*, *534*, 478–492. https://doi.org/10.1016/j.jhydrol.2016.01.020

Dimitriou, E., Panagiotopoulos, I., Mentzafou, A., & Anagnostou, C. (2018). Assessing the anthropogenic impacts on the fluvial water and sediment fluxes into the Thermaikos gulf, northern Greece. *Environmental Engineering and Management Journal*, *17*(5), 1053–1068.

Dimitriou, E., & Stavroulaki, E. (2018). Assessment of Riverine Morphology and Habitat Regime Using Unmanned Aerial Vehicles in a Mediterranean Environment. *Pure and Applied Geophysics*, *175*(9), 3247–3261. https://doi.org/10.1007/s00024-018-1929-3

Ederle, S. (2017). *A simple raster-based model for floodplain inundation and uncertainty assessment Case study city Kulmbach*. Technical University of Munich.

Elkhrachy, I. (2018). Vertical accuracy assessment for SRTM and ASTER Digital Elevation Models: A case study of Najran city, Saudi Arabia. *Ain Shams Engineering Journal*, *9*(4), 1807–1817. https://doi.org/10.1016/j.asej.2017.01.007

European Environmental Agency. (2012). CORINE Land Cover CLC2012.

Fabris, L., Malcolm, I. A., Buddendorf, W. B., Millidine, K. J., Tetzlaff, D., & Soulsby, C. (2017). Hydraulic modelling of the spatial and temporal variability in Atlantic salmon parr habitat availability in an upland stream. *Science of the Total Environment*, *601–602*, 1046–1059. https://doi.org/10.1016/j.scitotenv.2017.05.112

Gallagher, S. P., & Gard, M. F. (1999). Relationship between chinook salmon (*Oncorhynchus tshawytscha*) redd densities and PHABSIM-predicted habitat in the Merced and Lower American rivers, California. *Canadian Journal of Fisheries and Aquatic Sciences*, *56*(4), 570–577. https://doi.org/10.1139/f98-198

García, A., Jorde, K., Habit, E., Caamaño, D., & Parra, O. (2011). Downstream environmental effects of dam operations: Changes in habitat quality for native fish species. *River Research and Applications*, *27*(3), 312–327. https://doi.org/10.1002/rra.1358

Goodell, C. (2014). *Breaking the HEC-RAS Code: A User's Guide to Automating HEC-RAS* (1st editio). Portland, OR: h2ls.

Grantham, T. E. (2013). USE OF HYDRAULIC MODELLING TO ASSESS PASSAGE FLOW CONNECTIVITY FOR SALMON IN STREAMS. *River Research and Applications*, *29*(2), 250–267. https://doi.org/10.1002/rra.1591

Horritt, M. S., & Bates, P. D. (2002). Evaluation of 1D and 2D numerical models for predicting river flood inundation. *Journal of Hydrology*, *268*(1–4), 87–99. https://doi.org/10.1016/S0022-1694(02)00121-X

Horritt, M. S., Bates, P. D., & Mattinson, M. J. (2006). Effects of mesh resolution and topographic representation in 2D finite volume models of shallow water fluvial flow. *Journal of Hydrology*, *329*(1–2), 306–314. https://doi.org/10.1016/j.jhydrol.2006.02.016

Hughes, W. (1993). Travel time in mountain basins. In C. Y. Kuo (Ed.), *Engineering Hydrology*. San Francisco: American Society of Civil Engineers. Retrieved from https://cedb.asce.org/CEDBsearch/record.jsp?dockey=0083353

Javernick, L., Brasington, J., & Caruso, B. (2014). Modeling the topography of shallow braided rivers using Structure-from-Motion photogrammetry. *Geomorphology*, *213*, 166–182. https://doi.org/10.1016/j.geomorph.2014.01.006

Jowett, I. G., & Duncan, M. J. (2012). Effectiveness of 1D and 2D hydraulic models for instream habitat analysis in a braided river. *Ecological Engineering*, *48*, 92–100. https://doi.org/10.1016/j.ecoleng.2011.06.036

Katopodis, C. C. (2012). Ecohydraulic approaches in aquatic ecosystems: Integration of ecological and hydraulic aspects of fish habitat connectivity and Suitability. *Ecological Engineering*, *48*, 1–7. https://doi.org/10.1016/j.ecoleng.2012.07.007

Kolden, E., Fox, B. D., Bledsoe, B. P., & Kondratieff, M. C. (2016). Modelling Whitewater Park Hydraulics and Fish Habitat in Colorado. *River Research and Applications*, *32*(5), 1116–1127. https://doi.org/10.1002/rra.2931

Kondolf, G. M., Larsen, E. W., & Williams, J. G. (2000). Measuring and Modeling the Hydraulic Environment for Assessing Instream Flows. *North American Journal of Fisheries Management*, *20*(4), 1016–1028. https://doi.org/10.1577/1548-8675(2000)020<1016:MAMTHE>2.0.CO;2

Küng, O., Strecha, C., Beyeler, A., Zufferey, J.-C., Floreano, D., Fua, P., & Gervaix, F. (2012). the Accuracy of Automatic Photogrammetric Techniques on Ultra-Light Uav Imagery. *ISPRS - International Archives of the Photogrammetry, Remote Sensing and Spatial Information Sciences*, *XXXVIII-1/*, 125–130. https://doi.org/10.5194/isprsarchives-XXXVIII-1-C22-125-2011

Lacey, R. W. J., & Millar, R. G. (2004). Reach scale hydraulic assessment of instream salmonid habitat restoration. *Journal of the American Water Resources Association*, *40*(6), 1631–1644. https://doi.org/10.1111/j.1752-1688.2004.tb01611.x

Leclerc, M., Boudreault, A., Bechara, T. A., & Corfa, G. (1995). Two-Dimensional Hydrodynamic Modeling: A Neglected Tool in the Instream Flow Incremental Methodology. *Transactions of the American Fisheries Society*, *124*(5), 645–662. https://doi.org/10.1577/1548-8659(1995)124<0645:TDHMAN>2.3.CO;2

Lee, J. H., Kil, J. T., & Jeong, S. (2010). Evaluation of physical fish habitat quality enhancement designs in urban streams using a 2D hydrodynamic model. *Ecological Engineering*, *36*(10), 1251–1259. https://doi.org/10.1016/j.ecoleng.2010.05.004

Lim, N. J., & Brandt, S. A. (2019). Flood map boundary sensitivity due to combined effects of DEM resolution and roughness in relation to model performance. *Geomatics, Natural Hazards and Risk*, *10*(1), 1613–1647. https://doi.org/10.1080/19475705.2019.1604573

Lin, Y. P., Lin, W. C., & Wu, W. Y. (2015). Uncertainty in various habitat suitability models and its impact on habitat suitability estimates for fish. *Water (Switzerland)*, *7*(8), 4088–4107. https://doi.org/10.3390/w7084088

Loukas, A., & Quick, M. C. (1996). Physically-based estimation of lag time for forested mountainous watersheds. *Hydrological Sciences Journal*, *41*(1), 1–19. https://doi.org/10.1080/02626669609491475

Md Ali, A., Solomatine, D. P., & Di Baldassarre, G. (2015). Assessing the impact of different sources of topographic data on 1-D hydraulic modelling of floods. *Hydrology and Earth System Sciences*, *19*(1), 631–643. https://doi.org/10.5194/hess-19-631-2015

Montgomery, D. R., & Buffington, J. M. (1997). Channel-reach morpohology in mountain drainage basins. *Gsa*, *109*(5), 596–612. https://doi.org/10.1130/0016-7606(1997)109<0596:CRMIMD>2.3.CO;2

Moore, K. M. S., & Gregory, S. V. (1988). Summer Habitat Utilization and Ecology of Cutthroat Trout Fry (Salmo clarki) in Cascade Mountain Streams. *Canadian Journal of Fisheries and Aquatic Sciences*, *45*(11), 1921–1930. https://doi.org/10.1139/f88-224

Mosley, P. M., & McKerchar, A. I. (1993). Streamflow. In D. R. Maidment (Ed.), *Handbook of Hydrology* (pp. 8.1-8.3.5). New York: McGraw-Hill.

Mouton, A. M., Schneider, M., Depestele, J., Goethals, P. L. M., & De Pauw, N. (2007). Fish habitat modelling as a tool for river management. *Ecological Engineering*, *29*(3), 305–315. https://doi.org/10.1016/j.ecoleng.2006.11.002

Overton, I. C., Smith, D. M., Dalton, J., Barchiesi, S., Acreman, M. C., Stromberg, J. C., & Kirby, J. M. (2014). Approche écosystémique et mise en œuvre de débits environnementaux dans la gestion intégrée des ressources en eau. *Hydrological Sciences Journal*, *59*(3–4), 860–877. https://doi.org/10.1080/02626667.2014.897408

Papadaki, C., Bellos, V., Ntoanidis, L., & Dimitriou, E. (2017). Comparison of West Balkan adult trout habitat predictions using a Pseudo-2D and a 2D hydrodynamic model. *Hydrology Research*, *48*(6), 1697–1709. https://doi.org/10.2166/nh.2016.352

Papadaki, C., Bellos, V., Stoumboudi, M., Kopsiaftis, G., & Dimitriou, E. (2017). Evaluation of streamflow habitat relationships using habitat suitability curves and HEC-RAS. *European Water*, *58*(November), 127–134. Retrieved from http://www.ewra.net/ew/pdf/EW_2017_58_19.pdf

Papadaki, C., Soulis, K., Muñoz-Mas, R., Martinez-Capel, F., Zogaris, S., Ntoanidis, L., & Dimitriou, E. (2016). Potential impacts of climate change on flow regime and fish habitat in mountain rivers of the south-western Balkans. *Science of the Total Environment*, *540*, 418–428. https://doi.org/10.1016/j.scitotenv.2015.06.134

Papaioannou, G. (2017). *Flood Hazard and Risk Modelling Framework for Ungauged Streams and Watersheds*. University of Thessaly.

Papaioannou, G., Efstratiadis, A., Vasiliades, L., Loukas, A., Papalexiou, S., Koukouvinos, A., … Kossieris, P. (2018). An Operational Method for Flood Directive Implementation in Ungauged Urban Areas. *Hydrology*, *5*(2), 24. https://doi.org/10.3390/hydrology5020024

Papaioannou, G., Loukas, A., & Georgiadis, C. (2013). The effect of riverine terrain spatial resolution on flood modeling and mapping. In *First International Conference on Remote Sensing and Geoinformation of the Environment (RSCy2013)* (Vol. 8795, p. 8). SPIE. https://doi.org/10.1117/12.2028218

Papaioannou, G., Loukas, A., Vasiliades, L., & Aronica, G. T. (2016). Flood inundation mapping sensitivity to riverine spatial resolution and modelling approach. *Natural Hazards*, *83*(1), 117–132. https://doi.org/10.1007/s11069-016-2382-1

Pasternack, G., & Senter, A. (2013). *21 st CENTURY INSTREAM FLOW ASSESSMENT FRAMEWORK FOR*

MOUNTAIN STREAMS. California. Retrieved from http://www.energy.ca.gov/2013publications/CEC-500-2013-059/CEC-500-2013-059.pdf

Patel, D. P., Ramirez, J. A., Srivastava, P. K., Bray, M., & Han, D. (2017). Assessment of flood inundation mapping of Surat city by coupled 1D/2D hydrodynamic modeling: a case application of the new HEC-RAS 5. *Natural Hazards*, *89*(1), 93–130. https://doi.org/10.1007/s11069-017-2956-6

Pix4D. (2019). How to automatically generate a Digital Terrain Model (DTM). Retrieved September 22, 2019, from https://support.pix4d.com/hc/en-us/articles/202560579-How-to-automatically-generate-a-Digital-Terrain-Model-DTM

Poff, N. L., Richter, B. D., Arthington, A. H., Bunn, S. E., Naiman, R. J., Kendy, E., … Warner, A. (2010). The ecological limits of hydrologic alteration (ELOHA): A new framework for developing regional environmental flow standards. *Freshwater Biology*, *55*(1), 147–170. https://doi.org/10.1111/j.1365-2427.2009.02204.x

Poff, N. L., & Schmidt, J. C. (2016). How dams can go with the flow. *Science*, *353*(6304), 1099–1100. https://doi.org/10.1126/science.aah4926

Poff, N. L., Tharme, R. E., & Arthington, A. H. (2017). Evolution of Environmental Flows Assessment Science, Principles, and Methodologies. In *Water for the Environment* (pp. 203–236). Elsevier. https://doi.org/10.1016/B978-0-12-803907-6.00011-5

R Core Team. (2014). R: A language and environment for statistical computing. Retrieved February 2, 2014, from https://www.r-project.org/

Schubert, J. E., Sanders, B. F., Smith, M. J., & Wright, N. G. (2008). Unstructured mesh generation and landcover-based resistance for hydrodynamic modeling of urban flooding. *Advances in Water Resources*, *31*(12), 1603–1621. https://doi.org/10.1016/j.advwatres.2008.07.012

Scott, D., & Shirvell, C. S. (1987). A critique of the Instream Flow Incremental Methodology and Observations on Flow Determination in New Zealand. In J. F. Craig & B. J. Kemper (Eds.), *Regulated Streams Advances in Ecology* (1st ed., p. 427). New York. https://doi.org/10.1007/978-1-4684-5392-8

SESAR. (2016). *European drones outlook study : Unlocking the value for Europe*. *Publication office of the European Union* (Vol. 136). https://doi.org/10.2829/085259

SMHI-HYPEweb. (2018). HYdrological Predictions for the Environment (SMHI - HYPEweb). Retrieved October 10, 2018, from http://hypeweb.smhi.se/explore/historical/time-series/europe/

Tamminga, A., Hugenholtz, C., Eaton, B., & Lapointe, M. (2015). Hyperspatial Remote Sensing of Channel Reach Morphology and Hydraulic Fish Habitat Using an Unmanned Aerial Vehicle (UAV): A First Assessment in the Context of River Research and Management. *River Research and Applications*, *31*(3), 379–391. https://doi.org/10.1002/rra.2743

Teng, J., Vaze, J., Dutta, D., & Marvanek, S. (2015). Rapid Inundation Modelling in Large Floodplains Using LiDAR DEM. *Water Resources Management*, *29*(8), 2619–2636. https://doi.org/10.1007/s11269-015-0960-8

Tonina, D., & Jorde, K. (2013). Approaches for Ecohydraulic Non-Numerical Models. In I. Maddock, A. Harby, P. Kemp, & P. Wood (Eds.), *Ecohydraulics: An Integrated Approach* (pp. 31–74). John Wiley & Sons, Ltd. https://doi.org/10.1002/9781118526576.ch3

Tsubaki, R., & Fujita, I. (2010). Unstructured grid generation using LiDAR data for urban flood inundation modelling. *Hydrological Processes*, *24*(11), 1404–1420. https://doi.org/10.1002/hyp.7608

Unger, M., Pock, T., Grabner, M., Klaus, A., & Bischof, H. (2009). A Variational Approach to Semiautomatic

Generation of Digital Terrain Models BT - Advances in Visual Computing. In G. Bebis, R. Boyle, B. Parvin, D. Koracin, Y. Kuno, J. Wang, … D. Coming (Eds.) (pp. 1119–1130). Berlin, Heidelberg: Springer Berlin Heidelberg.

van Oorschot, M., Kleinhans, M., Buijse, T., Geerling, G., & Middelkoop, H. (2018). Combined effects of climate change and dam construction on riverine ecosystems. *Ecological Engineering*, *120*(June), 329–344. https://doi.org/10.1016/j.ecoleng.2018.05.037

Vezza, P., Parasiewicz, P., Spairani, M., & Comoglio, C. (2014). Habitat modeling in high-gradient streams: The mesoscale approach and application. *Ecological Applications*, *24*(4), 844–861. https://doi.org/10.1890/11-2066.1

Vozinaki, A. E. K., Morianou, G. G., Alexakis, D. D., & Tsanis, I. K. (2017). Comparing 1D and combined 1D/2D hydraulic simulations using high-resolution topographic data: a case study of the Koiliaris basin, Greece. *Hydrological Sciences Journal*, *62*(4), 642–656. https://doi.org/10.1080/02626667.2016.1255746

Waddle, T. (2009). Field evaluation of a two-dimensional hydrodynamic model near boulders for habitat calculation. *River Research and Applications*, *30*(2), n/a-n/a. https://doi.org/10.1002/rra.1278

Wang, W., Gao, Y., Iribarren Anacona, P., Lei, Y., Xiang, Y., Zhang, G., … Lu, A. (2018). Integrated hazard assessment of Cirenmaco glacial lake in Zhangzangbo valley, Central Himalayas. *Geomorphology*, *306*, 292–305. https://doi.org/10.1016/j.geomorph.2015.08.013

Williams, R. D., Brasington, J., Vericat, D., & Hicks, D. M. (2014). Hyperscale terrain modelling of braided rivers: fusing mobile terrestrial laser scanning and optical bathymetric mapping. *Earth Surface Processes and Landforms*, *39*, 167–183. https://doi.org/10.1002/esp.3437

Woodget, A. S., Austrums, R., Maddock, I. P., & Habit, E. (2017). Drones and digital photogrammetry: from classifications to continuums for monitoring river habitat and hydromorphology. *Wiley Interdisciplinary Reviews: Water*, *4*(4), e1222. https://doi.org/10.1002/wat2.1222

Zogaris, S., Tachos, V., Economou, A. N., Chatzinikolaou, Y., Koutsikos, N., & Schmutz, S. (2018). A model-based fish bioassessment index for Eastern Mediterranean rivers: Application in a biogeographically diverse area. *Science of the Total Environment*, *622–623*, 676–689. https://doi.org/10.1016/j.scitotenv.2017.11.293

TABLE 1. Absolute camera position and orientation uncertainties

	X [m]	Y [m]	Z [m]	Omega [degree]	Phi [degree]	Kappa [degree]
Mean	0.137	0.138	0.249	0.054	0.057	0.029
Sigma	0.029	0.030	0.037	0.003	0.002	0.000

TABLE 2. Hydraulic-hydrodynamic modelling 2D flow area characteristics.

Mesh size (m)	Number of Elements	Average element size (m^2)
0.3	347146	0.09
0.5	124745	0.25
1	31048	1
1.6	12064	2.6
2.5	4902	6.39
3	3393	9.23

TABLE 3. Hydraulic-hydrodynamic modelling geometry configuration sets

SensComb		SensDTM		SensMesh	
DTM Resolution [m]	**Mesh Resolution [m]**	**DTM Resolution [m]**	**Mesh Resolution [m]**	**DTM Resolution [m]**	**Mesh Resolution [m]**
0.3	0.3	0.3	0.3	0.15	0.3
0.5	0.5	0.5	0.3	0.15	0.5
1	1	1	0.3	0.15	1
1.6	1.6	1.6	0.3	0.15	1.6
2.5	2.5	2.5	0.3	0.15	2.5
3	3	3	0.3	0.15	3

TABLE 4. Summary of WUA and WUA0.5 values for all examined hydraulic-hydrodynamic geometry configurations and all fish species combinations.

DTM and Mesh Resolution [m] / Scenarios	WUA [m^2]					WUA$_{0.5}$ [m^2]				
	Large Barbel	Large Trout	Small Barbel	Small Trout	Interquartile Range	Large Barbel	Large Trout	Small Barbel	Small Trout	Interquartile Range
	SensComb									
0.3	1509	1565	756	1479	225	1063	1015	358	800	338
0.5	1543	1599	769	1502	239	1085	1035	356	803	356
1	1653	1706	814	1582	276	1159	1135	365	848	414
1.6	1693	1792	854	1633	280	1218	1214	379	903	443
2.5	1951	1944	923	1774	385	1469	1395	430	1016	544
3	2120	2038	1021	1902	377	1632	1546	527	1217	522
DTM Resolution [m] / Scenarios	SensDTM									
0.3	1509	1566	756	1479	225	1063	1015	358	800	338
0.5	1492	1557	757	1472	215	1041	1001	358	787	331
1	1473	1552	763	1463	205	1013	1004	370	770	336
1.6	1448	1534	764	1450	194	983	978	378	753	320
2.5	1502	1596	815	1527	214	1009	1024	418	812	299
3	1677	1731	901	1672	211	1218	1193	490	993	332
Mesh Resolution [m] / Scenarios	SensMesh									
0.3	1512	1569	758	1481	226	1066	1021	358	803	341
0.5	1569	1613	773	1515	251	1115	1059	360	822	366
1	1625	1693	796	1550	280	1153	1125	359	846	408
1.6	1665	1757	819	1596	286	1175	1185	358	871	435
2.5	1709	1792	820	1610	318	1199	1238	346	894	452
3	1767	1854	850	1656	334	1254	1326	364	969	454

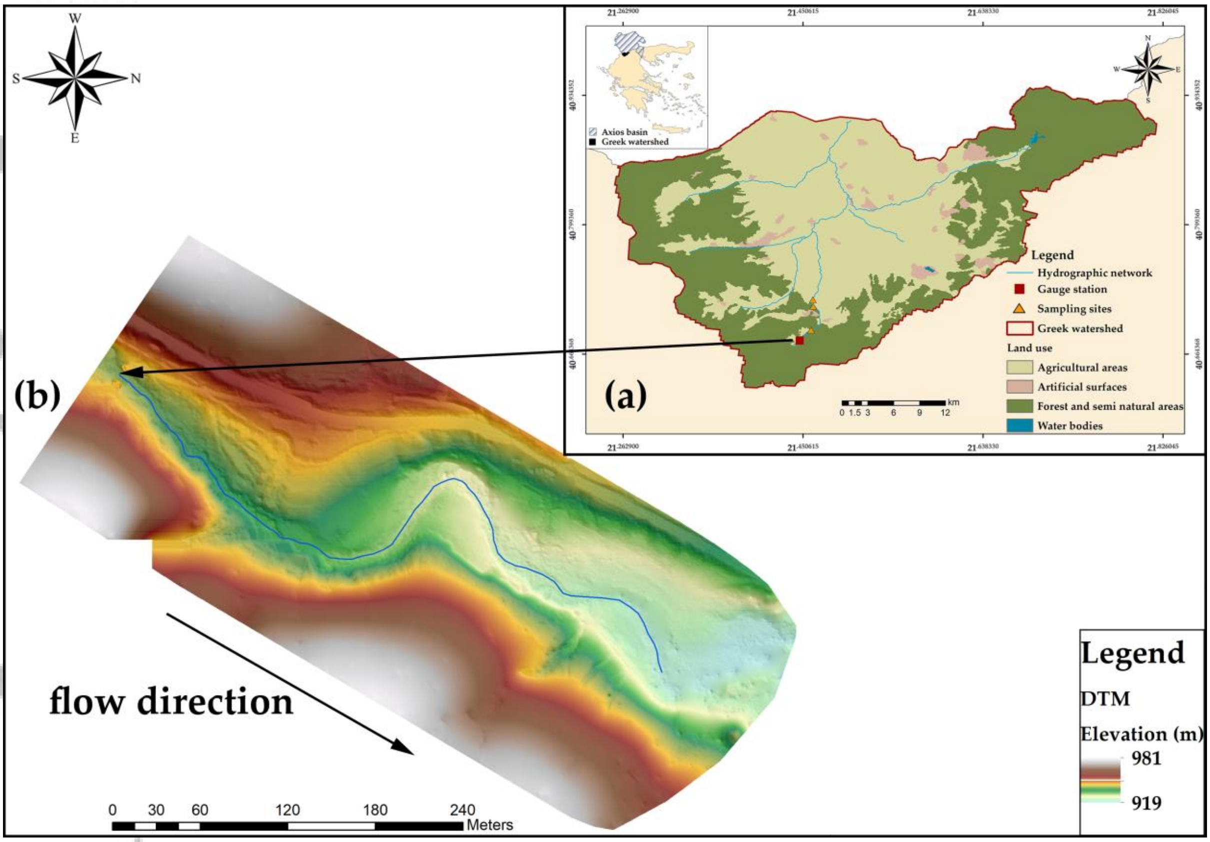

FIGURE 1. Study area: a) Greek watershed of Axios river. b) Terrain of the study area.

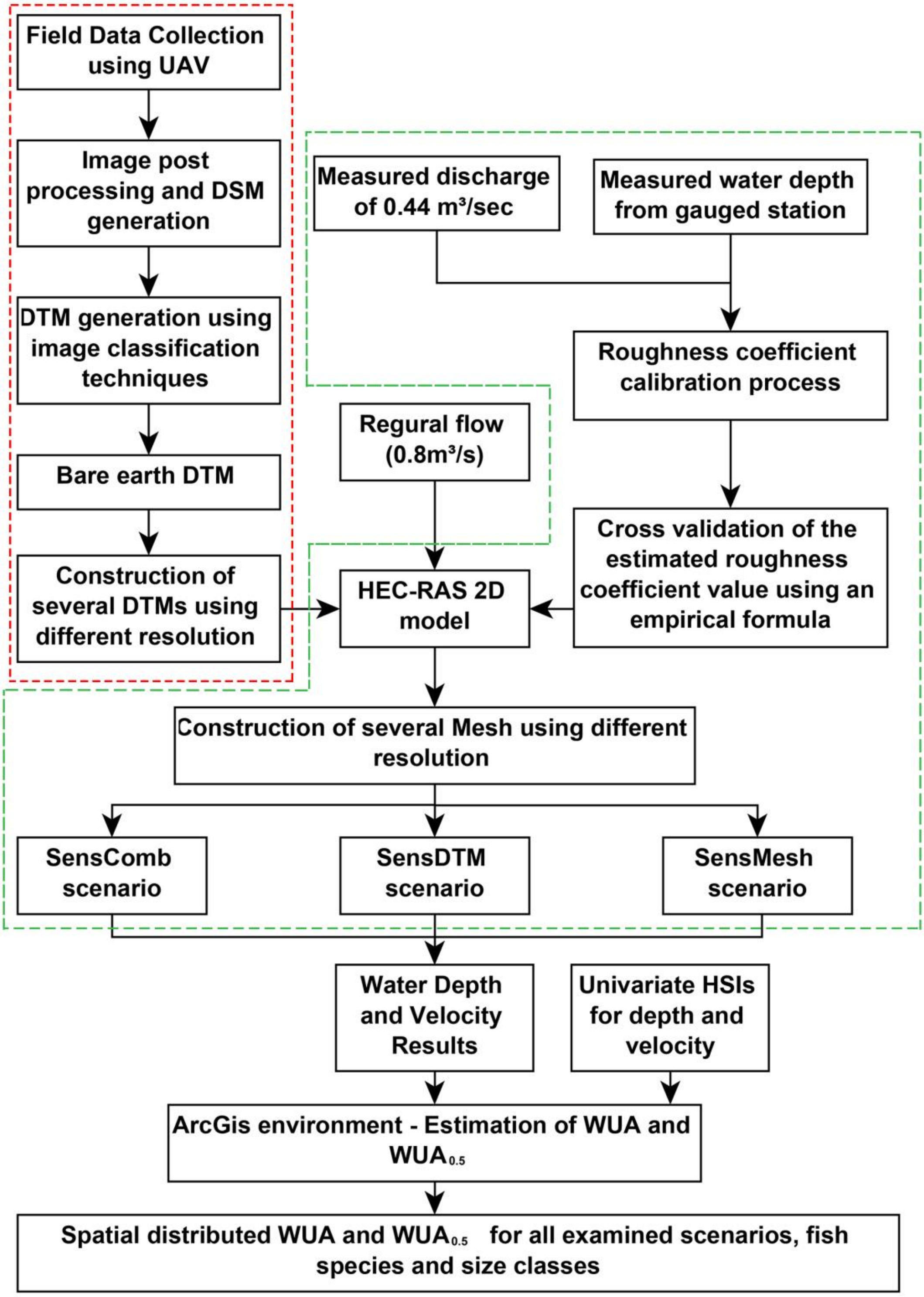

FIGURE 2. Flow chart of the applied methodology. Dashed red line - field data collection section, Dashed green line – Hydraulic-Hydrodynamic model section, Remaining elements – Habitat-Hydraulic modelling section.

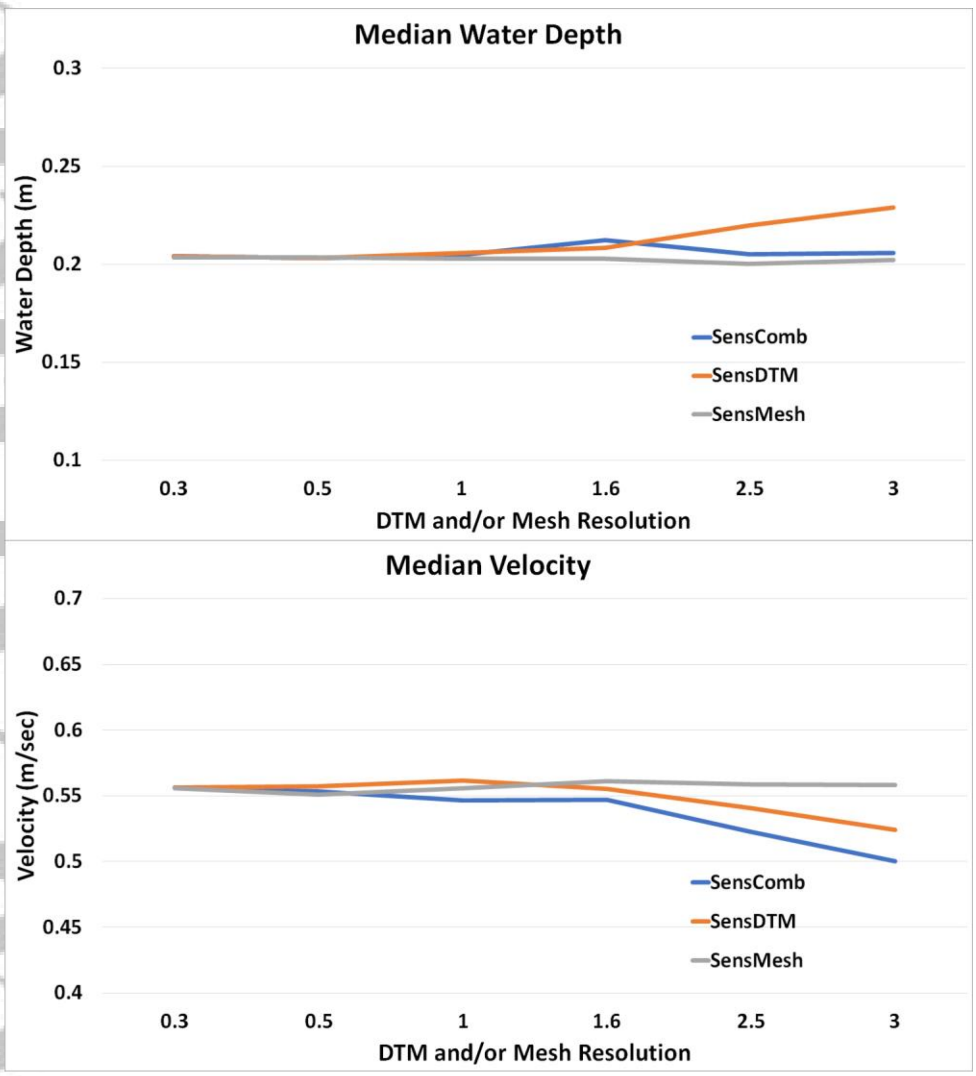

FIGURE 3. Median values of simulated water depth and velocity for all examined scenarios.

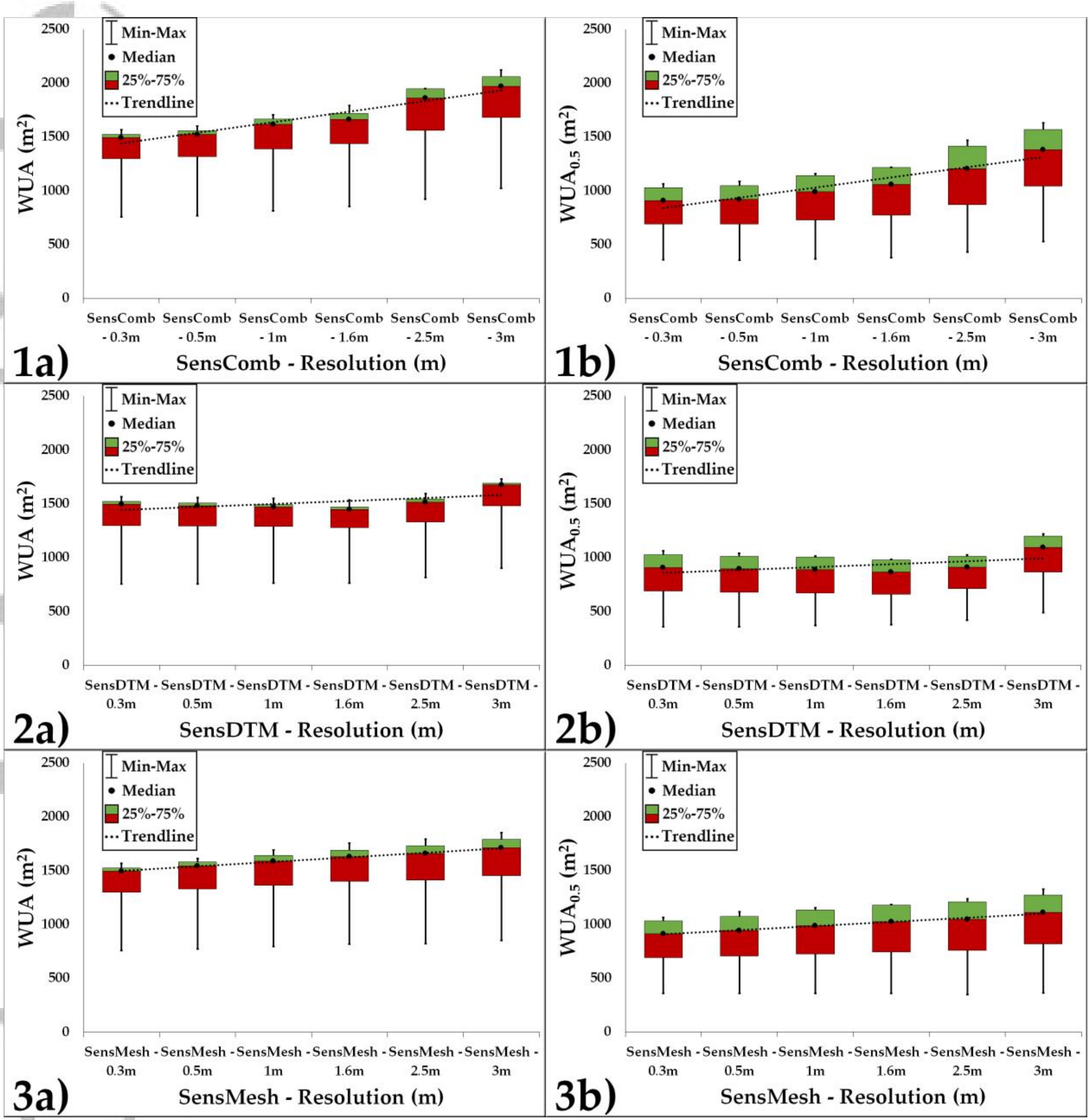

FIGURE 4. Box and Whisker plots according to WUA and WUA0.5 for all examined scenarios. The number of the graphs denote the hydraulic-hydrodynamic geometry scenarios [1) SensComb scenario, 2) SensDTM scenario, 3) SensMesh scenario], while the letter of the graphs denotes the two indices [a) WUA, b) WUA0.5].

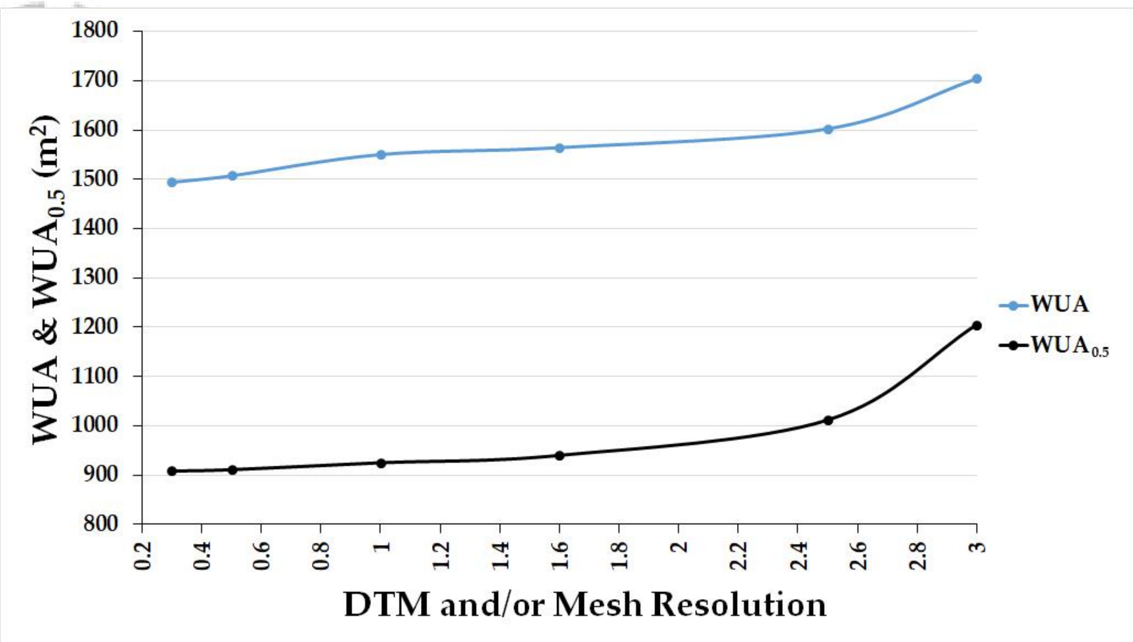

FIGURE 5. Median values of WUA and WUA0.5 that take into account all hydraulic-hydrodynamic geometry configurations in combination with all fish species combinations.

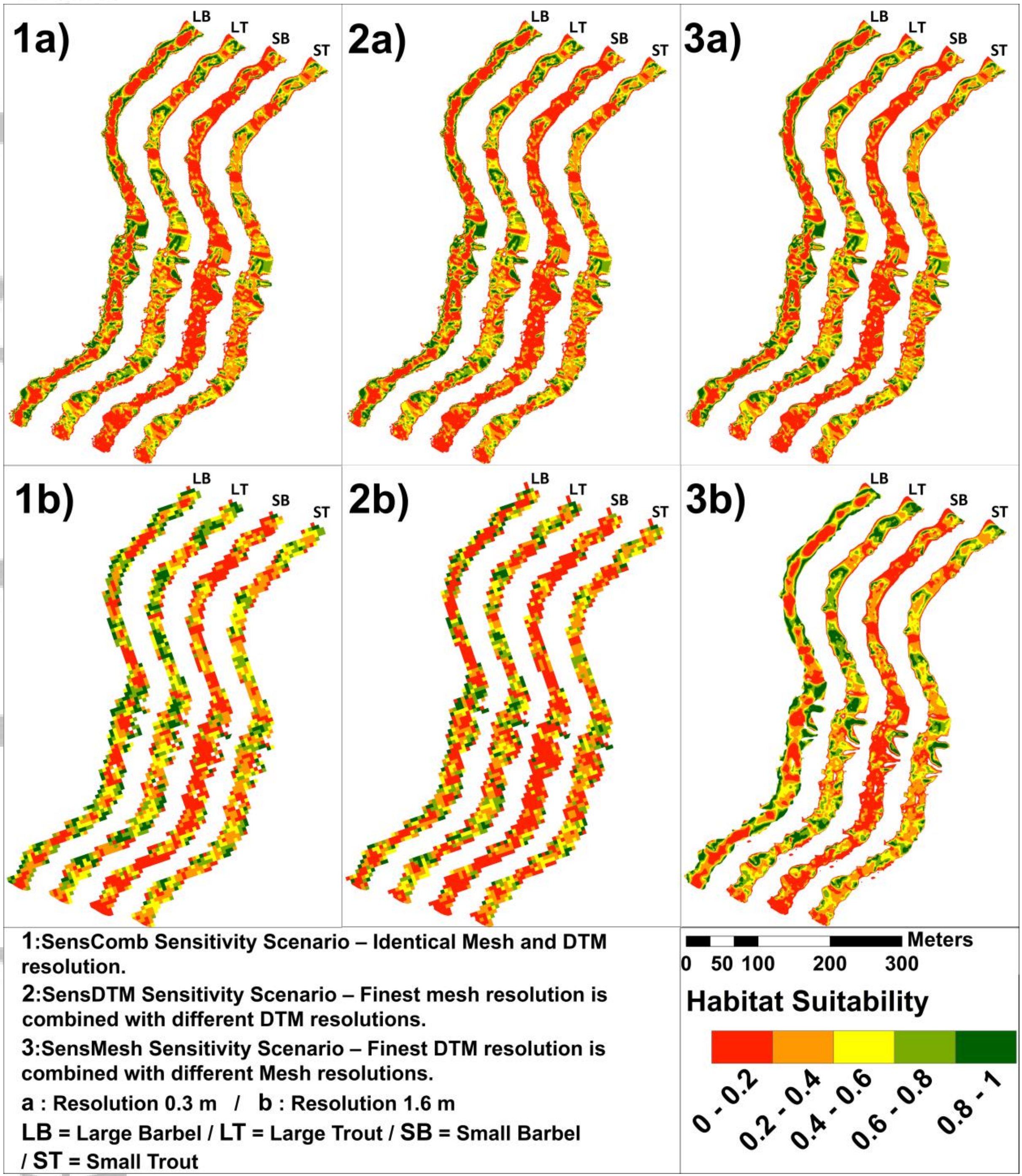

FIGURE 6. Visualization of the spatial distributed WUA for a part of the stream.

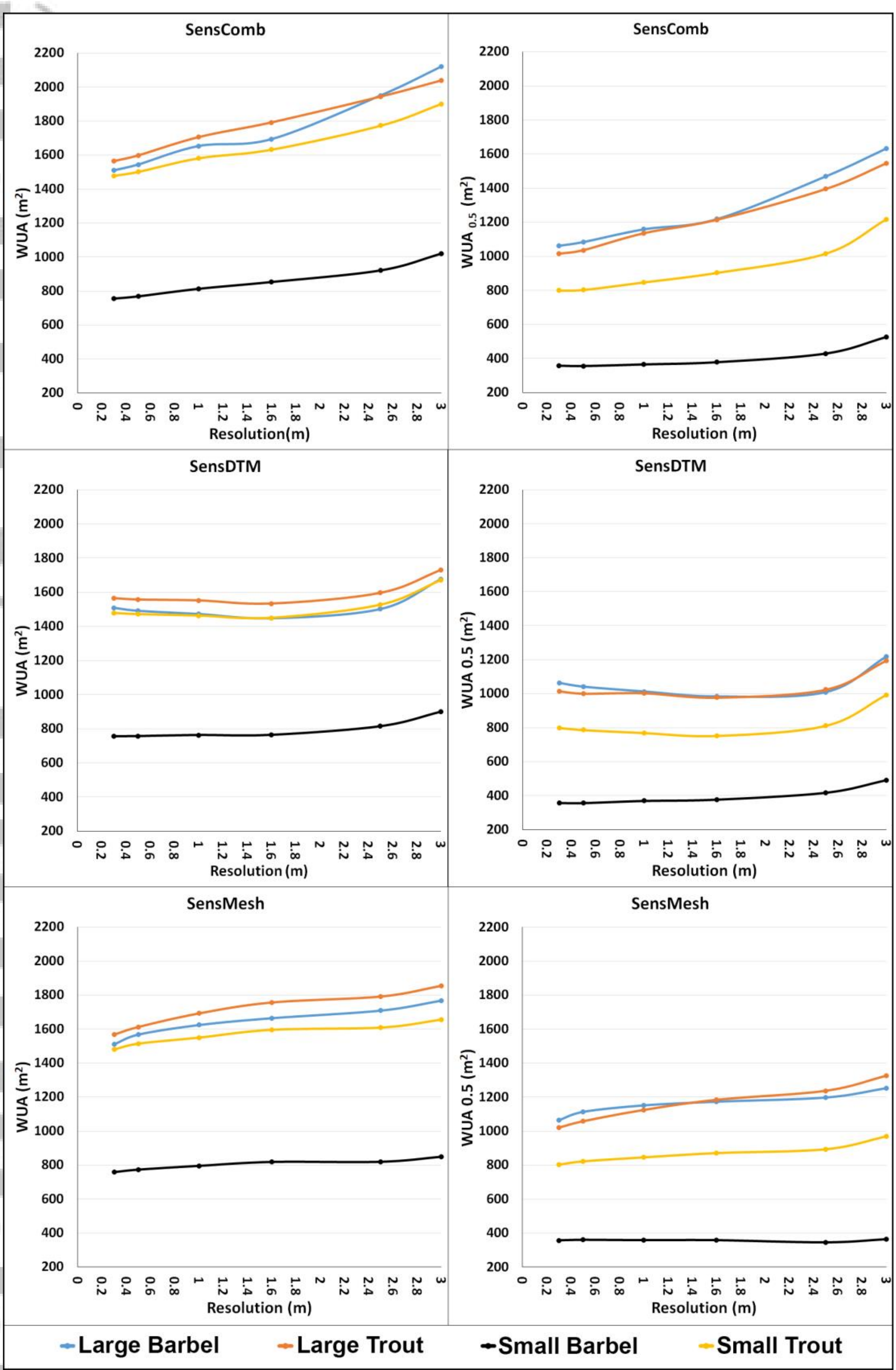

FIGURE 7. Graphical representation of WUA and WUA0.5 values, for all hydraulic-hydrodynamic geometry configurations and both fish species and sizes.